Journal of Neuroscience Research 83:1028–1038 (2006)

Influence of Caloric Restriction on Motor Behavior, Longevity, and Brain Lipid Composition in Sandhoff Disease Mice

Christine A. Denny,[1] Julie L. Kasperzyk,[1] Kristen N. Gorham,[1] Roderick T. Bronson,[2] and Thomas N. Seyfried[1]*

[1]Department of Biology, Boston College, Chestnut Hill, Massachusetts
[2]The Dana-Farber Cancer Institute/Harvard Medical School, Boston, Massachusetts

Caloric restriction (CR), which improves health and increases longevity, was studied as a therapy in a hexosaminidase β knockout mouse model of Sandhoff disease (SD), an incurable neurodegenerative disease involving accumulation of brain ganglioside GM2 and asialo-GM2 (GA2). Adult mice were fed a rodent chow diet either ad libitum (AL) or restricted to reduce body weight by 15–18% (CR). Although GM2 and GA2 were elevated, no significant differences were seen between the *Hexb*–/– and the *Hexb*+/– mice for most brain phospholipids and cholesterol. Cerebrosides and sulfatides were reduced in the *Hexb*–/– mice. In addition, rotorod performance was significantly worse in the *Hexb*–/– mice than in the *Hexb*+/– mice. CR, which decreased circulating glucose and elevated ketone bodies, significantly improved rotorod performance and extended longevity in the *Hexb*–/– mice but had no significant effect on brain lipid composition or on cytoplasmic neuronal vacuoles. The expression of CD68 and F4/80 was significantly less in the CR-fed than in the AL-fed *Hexb*–/– mice. We suggest that the CR delays disease progression in SD and possibly in other ganglioside storage diseases through anti-inflammatory mechanisms.

Key words: inflammation; ganglioside; ketone; rotorod; glucose; neurodegeneration

Sandhoff disease (SD) is an incurable glycosphingolipid (GSL) storage disorder that involves primarily the storage of ganglioside GM2 and its asialo derivative GA2 in brain and visceral tissues. The gangliosides are a family of sialic acid-containing glycosphingolipids (GSL) enriched in neuronal membranes and are involved in cell–cell and cell–matrix interactions (Ledeen, 1983). GM2 storage in SD occurs largely in neuronal lysosomes and leads to progressive neurodegeneration and brain dysfunction (Neufeld, 1991; Gravel et al., 1995). Reduction of cerebrosides and sulfatides, associated with dysmyelination, also accompanies GM2 accumulation (Sandhoff et al., 1971). SD is inherited as an autosomal recessive disorder as a result of pathogenic mutations in the lysosomal hexosaminidase β subunit, which contributes to the quaternary structure of both hexosaminidase A (Hexa) and hexosaminidase B (Hexb) isoenzymes. Patients with SD lack both the *Hexa* and *Hexb* isoenzymes, unlike patients with Tay-Sachs disease, who lack *Hexa*. The failure to catabolyze GM2 to GM3 in lysosomes is characteristic of both disorders (Sandhoff and Kolter, 2003).

A mouse model of SD, deficient in *Hexb* activity, was generated by using homologous recombination and embryonic stem cell technology (Sango et al., 1995). These mice mimic the pathological, biochemical, and clinical abnormalities of the human disease and can be used to explore new therapeutic approaches. Similarly to SD patients, the *Hexb*-deficient mice have a rapidly progressive neurodegenerative course that can facilitate associations among neurochemical pathology, behavior, and lipid storage (Sango et al., 1995; Phaneuf et al., 1996; Jeyakumar et al., 2003). We recently showed that these mice accumulate GM2 and GA2 in the brain as early as postnatal day 5 (p-5), thus mimicking the neurochemical features of the infantile disease form (Baek et al., 2004). However, *Hexb*-deficient mice are phenotypically indistinguishable from normal mice until adult ages, unlike infantile-onset SD patients, in whom ganglioside accumulation leads to behavioral and developmental abnormalities within the first few years of life. The *Hexb*-deficient mice have been used to evaluate therapies for reducing GSL storage to include bone marrow transplantation (BMT); enzyme replacement therapy (ERT); substrate reduction therapy (SRT), which aims to decrease the rate of GSL biosynthesis to counterbalance the impaired rate of catabolism; gene therapy; and, most recently, stem cell therapy (Norflus et al.,

Contract grant sponsor: NIH; Contract grant number: HD39722; Contract grant sponsor: Boston College Research Expense Fund; Contract grant sponsor: National Tay-Sachs and Allied Disease Association, Inc. (NTSAD).

*Correspondence to: Thomas N. Seyfried, PhD, Biology Department, Boston College, Chestnut Hill, MA 02467.
E-mail: thomas.seyfried@bc.edu

Received 24 October 2005; Revised 29 December 2005; Accepted 29 December 2005

Published online 6 March 2006 in Wiley InterScience (www.interscience.wiley.com). DOI: 10.1002/jnr.20798

1998; Jeyakumar et al., 1999, 2004; Kasperzyk et al., 2004; Baek et al., 2005; Arfi et al., 2005).

Neurodegeneration in SD involves microglial activation, macrophage infiltration, and oxidative damage (Wada et al., 2000). These changes are also associated with increased apoptosis and expression of inflammatory markers, including CD68 and F4/80 (Jeyakumar et al., 2003). It is not clear, however, the extent to which the neurodegeneration in SD results from pathological GSL accumulation or from neuroinflammation that accompanies this accumulation. Recent studies in SD mice show that nonsteroidal anti-inflammatory drugs (NSAIDs) increase life span and improve motor behavior associated with disease progression, suggesting that inflammation by itself contributes to disease pathogenesis (Jeyakumar et al., 2004). Furthermore, the combination of NSAIDs with SRT using *N*-butyldeoxynojirimycin (*N*B-DNJ) had additive effects on disease progression. These findings indicate that combinatorial therapies, which target both GSL storage and inflammation, may be more effective in influencing pathophysiology than either therapy alone.

CR has long been recognized as a natural therapy that improves health and extends longevity in humans and rodents (Weindruch and Walford, 1988; Greene et al., 2001, 2003; Duan et al., 2003; Koubova and Guarente, 2003). CR also has neuroprotective effects in rodent models of neurodegenerative diseases (Mattson, 2003). CR is produced from a total dietary restriction and differs from acute fasting or starvation in that CR reduces total caloric energy intake without causing anorexia or malnutrition (Mantis et al., 2003; Seyfried et al., 2004). CR diminishes neuroinflammation and oxidative stress that occur from aging by decreasing the production of reactive oxygen species and glial activation (Morgan et al., 1999; Lee et al., 2000). The neuroprotective effects of CR likely result from reduced glucose levels and elevated ketone bodies (β-OHB), which reduces oxygen free radicals and increases the $\Delta G'$ of ATP hydrolysis (Greene et al., 2003; Mantis et al., 2003; Veech, 2004).

In this study, we investigated the effects of CR in a mouse model of SD (*Hexb*–/– mice) during a period of severe disease progression (100–125 days of age). Our results show that CR significantly improved motor performance and extended longevity in the *Hexb*–/– mice but had no major effects on brain lipid composition or cytoplasmic neuronal vacuoles. Moreover, CR reduced expression of the inflammatory markers CD68 and F4/80. We suggest that CR may be a palliative therapy for SD and other ganglioside storage diseases. A preliminary report of these findings was recently published in abstract form (Denny et al., 2005).

MATERIALS AND METHODS

Mice

Mice heterozygous for the *Hexb* gene (*Hexb*+/–) were provided by Dr. Richard Proia (National Institutes of Health, Bethesda, MD). The mice were derived by homologous recombination and embryonic stem cell technology (Sango et al., 1995). *Hexb*+/+, *Hexb*+/–, and *Hexb*–/– mice were generated by crossing either a *Hexb*+/– or a *Hexb*–/– female with either a *Hexb*+/– or a *Hexb*–/– male. Genotypes were determined by measuring hexosaminidase-specific activity in tail tissue using a modification of the Galjaard procedure, as previously described (Galjaard, 1980; Hauser et al., 2004). *Hexb*+/? was used to designate mice that were either *Hexb*+/– or *Hexb*+/+. All mice were propagated in the Boston College Animal Care Facility and were housed individually in plastic cages with filter tops containing Sani-Chip bedding (P.J. Murphy Forest Products Corp., Montville, NJ). The room was maintained at 22°C on a 12-hr light/12-hr dark cycle. All animals were provided with cotton nesting pads for the duration of the experiment. All animal experiments were carried out with ethical committee approval in accordance with the National Institutes of Health *Guide for the care and use of laboratory animals* and were approved by the Institutional Animal Care Committee.

Caloric Restriction

All mice received Prolab RMH 3000 chow (LabDiet, Richmond, IN). The diet contains a balance of mouse nutritional ingredients and delivers 4.4 kcal g^{-1} gross energy, where fat, carbohydrate, protein, and fiber comprised 55, 520, 225, and 45 g kg^{-1} of the diet, respectively. After a 10-day pretrial period, the mice were placed into two groups (n = 4–5 mice/group) in which the average body weight of each *Hexb*–/– group was similar. At 100 days of age, the mice were assigned to either a control group that was fed standard lab chow ad libitum (AL) or an experimental group that was fed the same diet in restricted amounts (CR). Each mouse in the CR group served as its own control for body weight reduction. Based on food intake and body weight during the pretrial period, food in the CR-fed group was gradually reduced until each mouse achieved the target weight reduction of 15–18%. This was comparable to an approximate 30–35% reduction in calories per day. Body weight was used as an independent variable to reduce the variability among individual mice for the effects of caloric restriction (Pugh et al., 1999; Greene et al., 2001; Mantis et al., 2004). The target body weight reduction for all CR-fed *Hexb*–/– mice was reached in approximately 8 days.

The mice in the AL-fed group received 80 g of food in the hopper every 2 days between 1 PM and 3 PM as in the pretrial period. Daily food intake was estimated as the difference in food weight after 2 days divided by 2. Weighed food pellets were dropped directly into each cage for the CR-fed *Hexb*–/– mice and for the AL-fed *Hexb*–/– mice that developed motor deficiency as the study progressed.

Measurement of Plasma Glucose and β-Hydroxybutyrate

Mice were anesthetized with isoflurane (Halocarbon Laboratories, River Edge, NJ) and euthanized by exsanguination, involving collection of blood from the heart in heparinized tubes. The blood was centrifuged at 6,000*g* for 10 min, the plasma was collected, and aliquots were stored at –80°C until analysis. Plasma glucose concentration was measured in a spectrophotometer using the Stanbio Enzymatic Glucose Procedure (Stanbio). The ketone body β-hydroxybutyrate (β-OHB) was

measured enzymatically in plasma with a modification of the Williamson et al. (1962) procedure.

Tissue Processing

After sacrifice by cardiac puncture at 125 days of age, brains were collected for lipid, protein, and histological analysis. The right hemisphere was weighed and stored at –80°C. A portion of this hemisphere was then lyophilized for lipid analysis. The remaining portion was used for RNA and protein determination. The left hemisphere was stored in formalin (Sigma, St. Louis, MO) at 4°C for histological analysis.

Rotorod

A rotorod apparatus, consisting of a knurled dowel fixed 10 cm above Sani-Chip bedding, was used to measure motor coordination and balance. After a 3-day pretrial training period, mice were assessed for motor behavior every 5 days from 100 to 125 days of age. Mice were placed on the rotating dowel at speeds of 20, 30, 40, 52, and 60 rpm, indicating the start time for the trial. A 30-sec interval was allowed between the two trials at a given speed, and a 2-min interval was given between different speeds. The maximal time allowed on the bar for each trial was 60 sec. The trial was terminated when the mouse fell off the bar or at 60 sec. The *Hexb*–/– mice, often clung or wrapped around the bar as a consequence of declining ambulatory ability due to disease progression. Whereas the time on bar may be dependent on motor coordination and balance, the bar wrapping behavior may be more dependent on strength and endurance.

Lipid Isolation, Purification, and Quantification

Total lipids were isolated and purified from lyophilized brain tissue by using modifications of previously described procedures (Seyfried et al., 1978; Hauser et al., 2004; Kasperzyk et al., 2004). Neutral and acidic lipids were separated by using DEAE-Sephadex (A-25; Pharmacia Biotech, Upsala, Sweden) column chromatography as previously described (Macala et al., 1983; Seyfried et al., 1984; Kasperzyk et al., 2005). The total lipid extract, suspended in solvent A ($CHCl_3$:CH_3OH:H_2O, 30:60:8 by vol), was then applied to a DEAE-Sephadex column (1.2 ml bed volume) that had been equilibrated with solvent A. The column was washed twice with 20 ml of solvent A, and the entire neutral lipid fraction, consisting of the initial eluent plus washes, was collected. This fraction contained cholesterol, phosphatidylcholine, phosphatidylethanolamine, plasmologens, ceramide, sphingomyelin, cerebrosides, and asialo-GM2 (GA2). The acidic lipids were then eluted from the column with 30 ml solvent B ($CHCl_3$:CH_3OH:0.8 M Na acetate, 30:60:8 by vol). This fraction contained the gangliosides and other less hydrophilic acidic lipids to include free fatty acids, cardiolipin, phosphatidylserine, phosphatidylinositol, phosphatidic acid, and sulfatides. The gangliosides were isolated and purified from other acidic lipids and analyzed by using the resorcinol assay as we previously described (Kasperzyk et al., 2005).

High-Performance Thin-Layer Chromatography

All lipids were analyzed qualitatively by high-performance thin-layer chromatograph (HPTLC) according to previously described methods (Ando et al., 1978; Seyfried et al., 1978; Macala et al., 1983; Kasperzyk et al., 2005). Lipids were spotted on 10- × 20-cm Silica gel 60 HPTLC plates (E. Merck, Darmstadt, Germany) using a Camag Linomat III auto-TLC spotter (Camag Scientific Inc., Wilmington, NC). To enhance precision, an internal standard (oleoyl alcohol) was added to the neutral and acidic lipid standards and samples as previously described (Macala et al., 1983; Kasperzyk et al., 2005). Purified lipid standards were purchased from Matreya Inc. (Pleasant Gap, PA) or Sigma (St. Louis, MO) or were a gift from Dr. Robert Yu (Medical College of Georgia, Augusta, GA). The HPTLC plates were sprayed with either the resorcinol-HCl reagent or the orcinol-H_2SO_4 reagent and heated at 95°C for 30 min to visualize gangliosides or GA2, respectively (Kasperzyk et al., 2005). For neutral or acidic phospholipids, the plates were developed to a height of either 4.5 cm or 6 cm, respectively, with chloroform:methanol:acetic acid:formic acid:water (35:15:6:2:1 by vol), then developed to the top with hexanes:diisopropyl ether:acetic acid (65:35:2 by vol) as previously described (Macala et al., 1983; Seyfried et al., 1984). Neutral and acidic lipids were visualized by charring with 3% cupric acetate in 8% phosphoric acid solution, followed by heating in an oven at 160–170°C for 7 min.

The percentage distribution of the individual lipid bands was determined by scanning the plates on a Personal Densitometer SI with ImageQuant software (Molecular Dynamics, Sunnyvale, CA) for gangliosides, acidic lipids, and neutral lipids or on a ScanMaker 4800 with ScanWizard5 V7.00 software (Microtek, Carson, CA) for GA2.

Histology

The formalin-fixed left hemispheres were embedded in paraffin, sectioned at 5 μm, and stained with hematoxylin & eosin (H&E), Luxol fast blue (LFB), and periodic acid Schiff (PAS) at the Harvard University Rodent Histopathology Core Facility (Boston, MA). Slides were examined by using a Zeiss Axioplane 2 Imaging universal microscope and a Spot Insight 4MP Fireware Color 3-shot digital camera and Spot software.

Immunohistochemistry

CD68 and F4/80 immunohistochemistry was analyzed via methods similar to those we previously described (Mukherjee et al., 1999, 2002). Briefly, brain tissue sections analyzed for CD68 were placed in 10 mM sodium citrate buffer, pH 6.0, at 95°C for 10 min. Slides were allowed to cool in the buffer for approximately 20 min and then washed. The sections were quenched with 0.3% H_2O_2-methanol for 30 min and then blocked with 10% normal donkey serum in 100 ml of 0.01 M phosphate and 0.9% sodium chloride (pH 7.4) with 1.0 g of bovine serum albumin and 0.1 ml Tween 20 (PBA buffer). The sections were then treated with an antibody to CD68 (1/50; Santa Cruz Biotechnology, Santa Cruz, CA), followed by a biotin-SP-conjugated AffiniPure donkey anti-goat IgG (H + L) at 1:100 dilution (Jackson Immunoresearch Laboratories, West Grove, PA). The sections were next treated with avidin-biotin complex, followed by a 3,3′-diaminobenzidine as substrate for staining according to the manufacturer's directions (Vectastain Elite ABC kit; Vector, Burlingame, CA). The sections were rinsed three times with PBS (0.01 M phosphate buffer with 0.9% NaCl), counterstained with Harris-modified hematoxylin with acetic acid

(Fisher, Fair Lawn, NJ), and mounted. A corresponding tissue section without primary antibody served as the negative control.

Brain tissue sections analyzed for F4/80 were placed in a solution of trypsin:water (1:1) for 30 min at 37°C. The sections were washed and blocked with PBS:serum (10:1) and treated with an antibody to F4/80 (1/100; Serotec Inc., Raleigh, NC), followed by a biotin-SP-conjugated AffiniPure goat anti-rat IgG (H + L) at 1:100 dilution (Vector). The sections were then treated with avidin-biotin complex, followed by a 3,3′-diaminobenzidine as substrate for staining according to the manufacturer's directions (Vectastain Elite ABC kit). The sections were rinsed three times with PBS (0.01 M phosphate buffer with 0.9% NaCl), counterstained with methyl green (Vector), and mounted. A corresponding tissue section without primary antibody served as the negative control.

Semiquantitative RT-PCR

Total RNA was isolated from brain tissue with Trizol Reagent (Invitrogen, La Jolla, CA), following the manufacturer's protocol. Spectrophotometric measurements at 260 and 280 nm determined RNA concentration and purity. Single-strand cDNA was synthesized from total RNA (3 μg) by using oligo (dT) primers (Promega, Madison, WI) in a 20-μl reaction with Moloney murine leukemia virus reverse transcriptase (M-MLV RT; Promega) according to the manufacturer's protocol. cDNA was used for PCR amplification of the 544-, 514-, and 497-bp regions of the CD68, β-actin, and F4/80 genes, respectively. The CD68 primers, based on Genbank NM_009853, amplified the region from nucleotides 95 to 638 (forward 5′-CAT CCT TCA CGA TGA CAC CTA CAG-3′ and reverse 5′-CTC TGA TGT AGG TCC TGT TTG AAT C-3′). The β-actin primers (forward 5′-TGT GAT GGT GGG AAT GGG TCA G-3′ and reverse 5′-TTT GAT GTC ACG CAC GAT TTC C-3′; based on GenBank NM_007393) amplified the region from nucleotides 207 to 719. The F4/80 primers (forward 5′-CCT ATC TGT GTC TCC TGG AAC-3′ and reverse 5′-GTG CAG CAT CTT GAT GTT GCG-3′; based on GenBank X93328) amplified the region from nucleotides 1,777 to 2,271. Amplicons were confirmed by sequence analysis, and Genbank numbers are DQ167574 and DQ167573 for CD68 and F4/80, respectively. Gradient PCR was performed to obtain optimal primer annealing temperatures (65°C, 58°C, and 61°C for CD68, β-actin, and F4/80, respectively). To determine the linear range for the amplification reaction, PCR was performed at increasing cycle numbers, and optimal PCR cycle number was determined to be 27 cycles, 22 cycles, and 27 cycles for CD68, β-actin, and F4/80, respectively. PCR amplification of CD68, β-actin, and F4/80 was performed with Taq DNA polymerase (Promega) with the following protocol: initial denaturation at 95°C for 2 min; followed by 27, 22, or 27 cycles, respectively; denaturation at 94°C for 1 min; annealing at 65°C, 58°C, and 61°C, respectively, for 25 sec; and extension at 72°C for 1 min. A final extension at 72°C for 6 min followed the last cycle for CD68, β-actin, and F4/80 amplifications. PCR products were separated on 0.8–1% agarose gels containing ethidium bromide, visualized with UV light, and analyzed in 1D Kodak software. RT-PCR was performed on the total RNA of each sample in the absence of reverse transcriptase to control for possible DNA contamination.

Statistical Analysis

A two-tailed *t*-test and the Pearson product-moment correlation were used to evaluate the significance of differences between the AL and the CR groups. In each figure, n designates the number of individual mice analyzed.

RESULTS

Hexb enzymatic activity was about 50% lower in the *Hexb*+/− mice than in the *Hexb*+/+ mice, but the mice were similar in behavior, brain lipid composition, and tissue histology. Therefore, data for the *Hexb*+/− mice and the *Hexb*+/+ mice were combined and are presented as a normal control group (*Hexb*+/? mice). No adverse effects were observed in the CR-fed *Hexb*−/− mice. Even with reduced body weight, the CR-fed *Hexb*−/− mice were healthier and more active than the AL-fed *Hexb*−/− mice as assessed by ambulatory, grooming, and nest-building behavior (data not shown). According to the standard criteria for mice, there were no signs of vitamin or mineral deficiency observed in the CR-fed *Hexb*−/− mice (Hoag and Dickie, 1968). These findings are consistent with the well-recognized health benefits of mild to moderate CR in rodents (Keenan et al., 1999).

Influence of CR on Body Weight

All mice were matched for age (90 days of age) before the start of the dietary treatment. The *Hexb*−/− mice were also matched for body weights (~27.5 g; Fig. 1A). These weights differed somewhat from those of *Hexb*+/? mice because of variability within and between litters. Whereas body weights remained relatively stable in the AL-fed *Hexb*+/? mice from 100 to 125 days of age, body weights in the AL-fed *Hexb*−/− mice remained relatively stable until 115 days of age and then dropped significantly as a result of disease progression. In the CR-fed *Hexb*−/− mice, body weight declined gradually until 110 days of age and then remained stable, similar to that of the *Hexb*+/? mice. These findings indicate that CR prevented the body weight decline associated with disease progression in the *Hexb*−/− mice. The standard error of the mean for body weight ranged from 0.230 to 2.061 from 100 to 125 days of age for all groups.

Influence of CR on Plasma Glucose and β-OHB Levels

Glucose levels were approximately 12 mM for both the AL-fed *Hexb*+/? and the AL-fed *Hexb*−/− mice but were significantly lower in the CR-fed *Hexb*−/− mice (Fig. 1B). Plasma β-OHB levels were approximately 0.25 mM for both the AL-fed *Hexb*+/? and the *Hexb*−/− mice but were significantly elevated in the CR-fed *Hexb*−/− mice (Fig. 1C). These findings are consistent with our previous studies showing that β-OHB levels are increased under CR and that circulating β-OHB levels are inversely related to circulating glucose levels (Greene et al., 2001; Mantis et al., 2004).

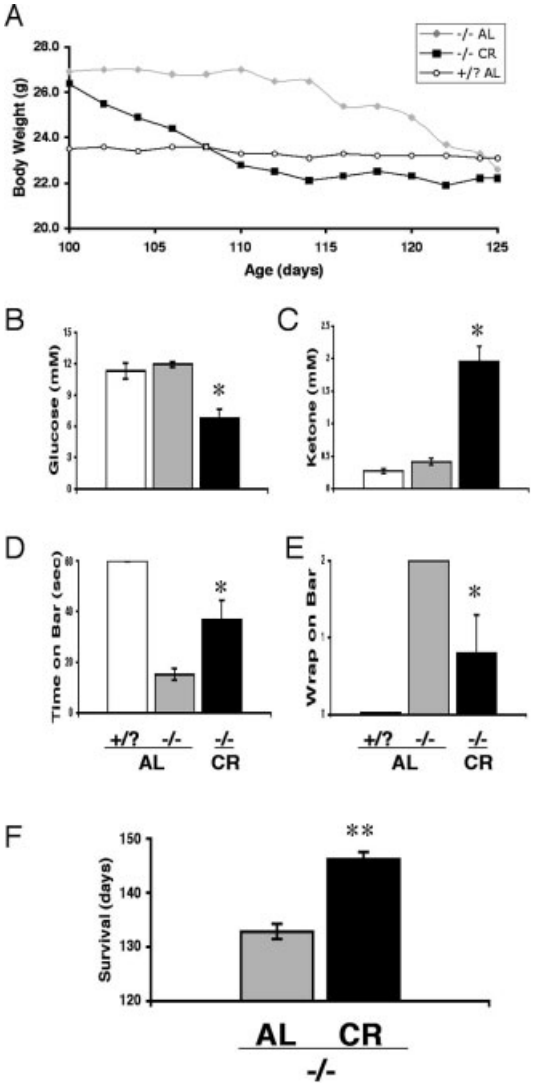

Fig. 1. Influence of CR on body weight (**A**), glucose (**B**), β-hydroxybutyrate (**C**), rotorod performance at 40 rpm (**D**), wrapping behavior at 40 rpm (**E**), and survival (**F**). Values are expressed as means (±SEM) and, 4–9 mice were analyzed in each group. Asterisks indicates that the value of the CR-fed *Hexb*–/– mice is significantly different from that of the AL-fed *Hexb*–/– mice at $*p < 0.05$ and $**p < 0.01$ as determined by the two-tailed *t*-test.

TABLE I. Influence of Caloric Restriction on Brain Ganglioside Content in Adult *Hexb* Mice[†]

Diet	Genotype	N[a]	Brain weight (mg)	Water content (%)	Ganglioside sialic acid (μg/100 mg dry wt.)
AL	+/?	3	71.9 ± 2.3	78.77 ± 0.26	458 ± 36
	–/–	4	73.6 ± 1.6	78.83 ± 0.27	732 ± 27★
CR	–/–	4	74.5 ± 4.3	77.26 ± 1.29	725 ± 12★

[†]Values represent mean ± SEM.
[a]N, number of independent mice analyzed.
★Significantly different from that of the control mice at $p < 0.01$ as determined by two-tailed *t*-test.

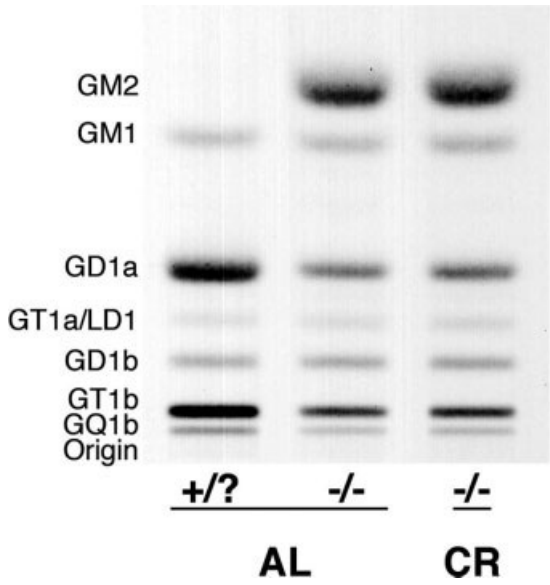

Fig. 2. HPTLC of brain gangliosides in adult *Hexb* mice. The amount of ganglioside sialic acid spotted per lane was equivalent to approximately 1.5 μg. The plate was developed by a single ascending run with $CHCl_3$:CH_3OH:dH_2O (55:45:10 by vol) containing 0.02% $CaCl_2$ $2H_2O$. The bands were visualized with resorcinol-HCl spray.

Influence of CR on Motor Behavior and Survival

The rotorod apparatus was used to measure motor coordination and balance. Unlike the *Hexb*+/? mice, the *Hexb*–/– mice exhibited an age-dependent deficit in motor coordination and balance. Time on bar (rotorod performance) was significantly shorter in the AL-fed *Hexb*–/– mice than in the AL-fed *Hexb*+/? mice (Fig. 1D). However, the time on bar was significantly longer in the CR-fed *Hexb*–/– mice than in the AL-fed *Hexb*–/– mice, indicating that CR improved motor behavior in this task. In contrast to the AL-fed *Hexb*–/– mice, whose performance deteriorated rapidly from 100 to 125 days of age, the performance in CR-fed *Hexb*–/– mice declined less rapidly (data not shown). The performance of the *Hexb*+/? mice was significantly better than that of the *Hexb*–/– mice at all speeds and did not change significantly over the course of the study.

Normal mice rarely wrap around the rotorod bar which indicates good motor control. Wrapping behavior was significantly greater in the AL-fed *Hexb*–/– mice than in the AL-fed *Hexb*+/? mice, indicating poor motor abilities (Fig. 1E). However, wrapping was significantly less in the CR-fed *Hexb*–/– mice than in the AL-fed *Hexb*–/– mice. In contrast to the *Hexb*+/? mice, which normally live for approximately 2 years, the AL-fed *Hexb*–/– mice died between 129 and 141 days of age. CR significantly increased survival by 9% in the *Hexb*–/– mice (Fig. 1F). Nest-building behavior was noticeably better in the CR-fed *Hexb*–/– mice than in AL-fed *Hexb*–/– mice according to nest ratings based on Broida and Sware's four-point

TABLE II. Influence of Caloric Restriction on Brain Ganglioside Distribution in Adult *Hexb* Mice[†]

			Concentration (μg sialic acid/100 mg dry weight)[b]						
Diet	Genotype	N[a]	GM2	GM1	GD1a	GT1a/LD1	GD1b	GT1b	GO1b
AL	+/?	3	–	60 ± 16	167 ± 13	14 ± 1.2	51 ± 13	135 ± 8	32 ± 2.7
	−/−	4	302 ± 15★	52 ± 9	156 ± 12	21 ± 0.8★	53 ± 7	123 ± 7	27 ± 1.0
CR	−/−	4	282 ± 11★	54 ± 10	161 ± 18	21 ± 0.2★	55 ± 7	125 ± 10	27 ± 2.3

[†]Values represent mean ± SEM.
[a]N, number of independent samples analyzed.
[b]Determined from densitometric scanning of HPTLC as shown in Figure 2.
★Significantly different from that of the *Hexb* +/? mice at $p < 0.01$ as determined from the two-tailed *t*-test.

scale (Broida and Sware, 1982; Bond et al., 2002; data not shown). These findings considered together indicate that CR improves motor behavior, prolongs longevity, and attenuates disease progression in the *Hexb*–/– mice.

Influence of CR on Brain Lipids

We next determined whether the CR-induced improvements in motor behavior and survival were associated with changes in brain ganglioside content and distribution in the *Hexb*–/– mice. Total brain ganglioside concentration was significantly higher in the *Hexb*–/– mice than in the *Hexb*+/? mice (Table I). CR caused no significant changes in total brain ganglioside concentration in the *Hexb*–/– mice. In addition, CR had no significant effect on brain weight or brain water content, a general marker for brain maturation (Seyfried et al., 1978). The influence of CR on the qualitative and quantitative distribution of individual gangliosides in the *Hexb* mice is shown in Figure 2 and Table II. In contrast to the *Hexb*+/? mice, in which GM2 content was present in only trace amounts, GM2 was the major ganglioside in the *Hexb*–/– mice. CR had no statistically significant effect on the content of GM2 or that of other gangliosides in the *Hexb*–/– mice. The data were also analyzed by using the Pearson product-moment correlation to determine whether changes in the GM2 content in each mouse were associated with changes in motor behavior (rotorod performance). The correlation coefficient for GM2 levels and rotorod performance was not significant ($r = 0.024$, 7 df, $P = 0.955$) further supporting the results from the two-tailed *t*-test. These findings indicate that the CR-induced improvement in motor behavior and survival in the *Hexb*–/– mice was not due to subtle changes in brain GM2 content.

The influence of CR on the qualitative and quantitative distribution of neutral and acidic brain lipids in the *Hexb* mice is shown in Figures 3 and 4 and Table III. Cerebrosides and sulfatides were significantly reduced in the AL-fed *Hexb*–/– mice when compared with the AL-fed *Hexb*+/? mice. GA2, on the other hand, was significantly elevated in the AL-fed *Hexb*–/– mice when compared with the *Hexb*+/? mice. With the exception of a slight, but significant, reduction in phosphatidylcholine ($P < 0.05$) in the *Hexb*–/– mice, no significant differences were observed between the *Hexb*+/? mice and the *Hexb*–/– mice for the distribution of other phospholipids or for ceramide. CR had no significant effect on the distribution of these lipids in the *Hexb*–/– mice. It is important to mention that the solvent front (SF) does not include lipids but rather slight impurities from the organic solvents used in the developing system. These findings indicate that CR improve motor behavior and longevity through marked effects on the content or distribution of major brain lipids.

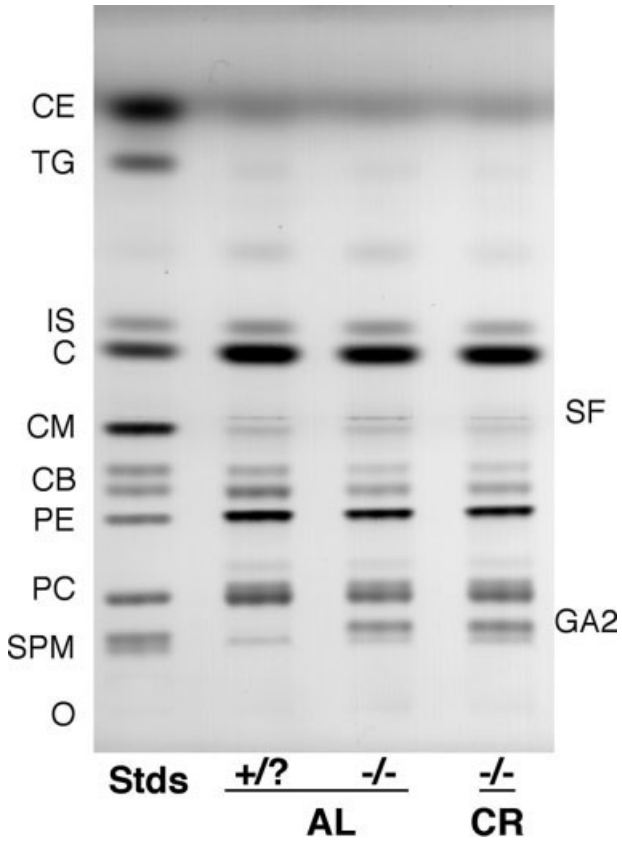

Fig. 3. HPTLC of brain neutral lipids in adult *Hexb* mice. The amount of neutral lipids spotted per lane was equivalent to approximately 70 μg tissue dry weight. The plates were developed as described in Materials and Methods. CE, cholesterol esters; TG, triglycerides; IS, internal standard; C, cholesterol; CM, ceramide; CB, cerebrosides (doublet); PE, phosphatidylethanolamine; PC, phosphatidylcholine; GA2, asialo-GM2; SPM, sphingomyelin; O, origin; and SF, solvent front of the first developing solvent system.

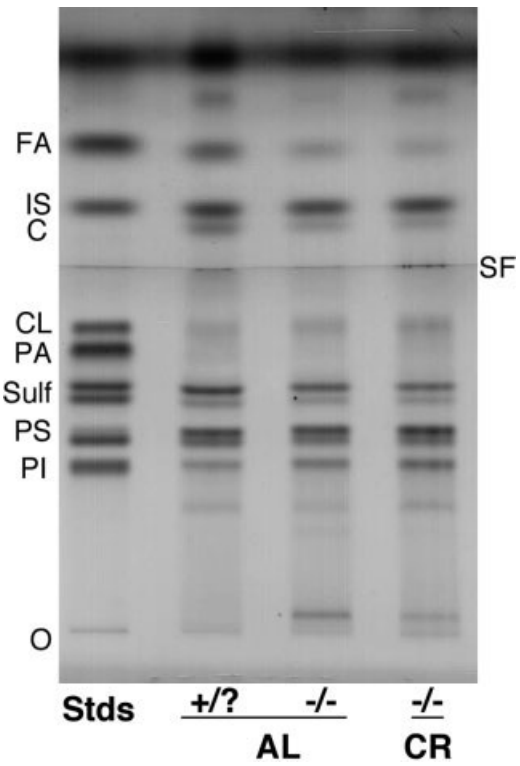

Fig. 4. HPTLC of brain acidic lipids in adult *Hexb* mice. The amount of acidic lipids spotted per lane was equivalent to approximately 200 μg tissue dry weight. The plates were developed as described in the Materials and Methods. FA, fatty acids; IS, internal standard; C, cholesterol; CL, cardiolipin; PA, phosphatidic acid; Sulf, sulfatides (doublet); PS, phosphatidylserine; PI, phosphatidylinositol, O, origin; and SF, solvent front of the first developing solvent system.

Influence of CR on Brain Histology

Sections of the cerebellum were stained with LFB to visualize lysosomal storage material (Fig. 5A). No LFB-positive storage material was detected in the brains of the AL-fed *Hexb*+/? mice. In contrast, noticeable LFB-positive storage vacuoles were seen in Purkinje cells in the AL-fed *Hexb*–/– mice. CR had no noticeable effects on the storage material in the *Hexb*–/– mice. Similar results were obtained with PAS, which also identifies cytoplasmic glycolipid storage material (data not shown). Sections of the nucleus gracilis were stained with H&E to analyze structural differences between the *Hexb*+/? mice and the *Hexb*–/– mice. Dystrophic neurons, a sign of neurodegeneration, were noticeably greater in the nucleus gracilis of the AL-fed *Hexb*–/– mice than in the AL-fed *Hexb*+/? mice (Fig. 5B). CR had no noticeable effect on the number of dystrophic neurons in the *Hexb*–/– mice. These findings indicate that CR does not noticeably reduce histological abnormalities in the *Hexb*–/– mice.

Influence of CR on CD68 and F4/80

CD68 is a major component of lysosomal membranes and is expressed on the surface of macrophages (Micklem et al., 1989). F4/80 is a 125-kDa transmembrane protein that is often expressed by a majority of mature macrophages (Austyn and Gordon, 1981). CD68 and F4/80 immunostaining was stronger in brain sections of the AL-fed *Hexb*–/– mice than in those of the AL-fed *Hexb*+/? mice (Fig. 6A,B). However, CD68 and F4/80 immunostaining was noticeably less in the CR-fed *Hexb*–/– mice than in the AL-fed *Hexb*–/– mice. The strongest staining appeared in cells with a neuronal morphology. The reduction in CD68 and F4/80 CNS immunostaining was also associated with significant reductions in CD68 and F4/80 gene expression in the CR-fed *Hexb*–/– mice (Fig. 6C,D). These findings indicate that CR reduces expression of inflammatory markers in the brains of *Hexb*–/– mice.

TABLE III. Influence of Caloric Restriction on Acidic and Neutral Brain Glycosphingolipids in Adult *Hexb* mice[†]

Diet	Genotype	Sulfatides[a] (mg/100 mg dry wt.)	Cerebrosides[a] (mg/100 mg dry wt.)	GA2[b] (mg/100 mg dry wt.)
AL	+/?	2.0 ± 0.1	2.0 ± 0.1	–
	–/–	1.5 ± 0.2★	1.3 ± 0.1★★	2.9 ± 0.2
CR	–/–	1.6 ± 0.1★	1.2 ± 0.1★★	2.7 ± 0.2

[†]Values represent mean ± SEM of three or four independent brain samples.
[a]Determined from densitometric scanning of HPTLC as shown in Figures 3 and 4.
[b]Determined from HPTLC analysis as described in Materials and Methods.
★$p < 0.05$ vs. *Hexb*+/? mice (two-tailed *t*-test).
★★$p < 0.01$ vs. *Hexb*+/? mice (two-tailed *t*-test).

DISCUSSION

CR is produced from a total restriction of dietary nutrients and differs from starvation in that CR reduces total caloric energy intake without causing anorexia or malnutrition (Tannenbaum et al., 1942, 1959; Weindruch et al., 1988; Kritchevsky, 1999; Mukherjee et al., 1999; Greene et al., 2003; Seyfried and Mukherjee, 2005). As a natural dietary therapy, CR improves health and longevity, is neuroprotective, and reduces inflammation (Weindruch et al., 1988; Greene et al., 2001, 2003; Chung et al., 2002; Duan et al., 2003; Spindler, 2005). No prior studies have evaluated the effects of CR on disease progression in a ganglioside storage disease. We found that CR significantly increased survival and attenuated disease progression in SD mice that accumulated large amounts of GM2 and GA2 in the brain. CR also significantly improved motor behavior and coordination in these mice.

Recent studies indicate that inflammation is a hallmark of the pathogenesis in ganglioside storage diseases, including SD (Myerowitz et al., 2002; Jeyakumar et al., 2003). This inflammatory phenotype consists of progressive microglial activation, macrophage recruitment, and proinflammatory cytokine production in the brain (Wada et al., 2000; Jeyakumar et al., 2003). Progressive macrophage activation also precedes neuronal apoptosis and the onset of neurological deterioration (Wu and Proia, 2004). Consistent with these findings, we found that expression of

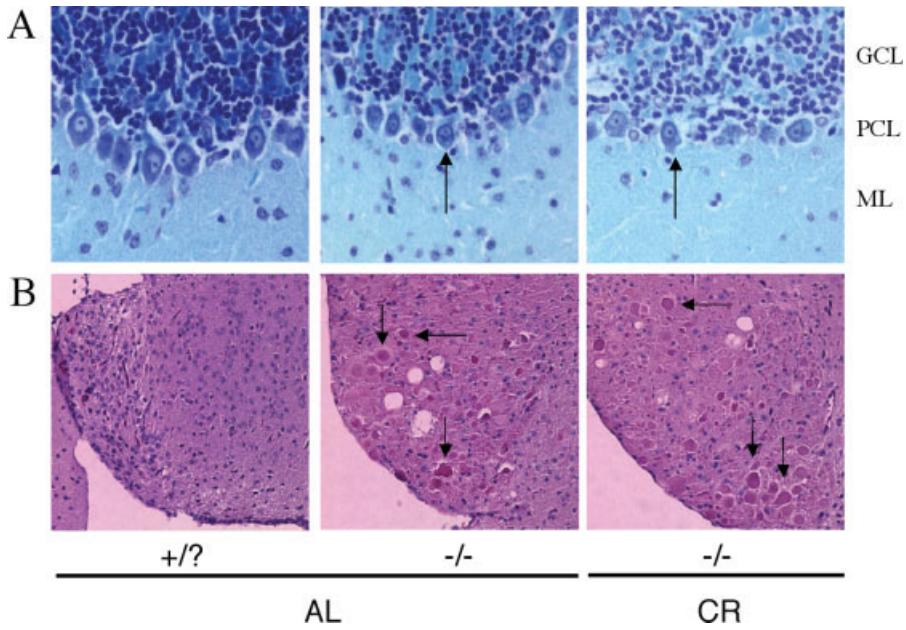

Fig. 5. LFB staining of Purkinje cells in the cerebellum of adult *Hexb* mice (**A**; sagittal, 5 μm). Images shown are 400×. Arrows indicated LFB positive storage vacuoles. GCL, granular cell layer; PCL, Purkinje cell layer; ML, molecular layer. H&E staining of the nucleus gracilis (**B**; sagittal, 5 μm). Images shown are 200×. Arrows indicate dystrophic axons. Figure can be viewed in color online via www.interscience.wiley.com.

CD68 and F4/80 was significantly higher in the brains of the *Hexb*−/− mice than in those of the *Hexb*+/? mice. Moreover, CR reduced expression of these inflammatory-associated markers in the *Hexb*−/− mice, suggesting that CR targets the inflammatory phenotype of SD. In addition, the number of apoptotic cells was markedly higher in the brains of the *Hexb*−/− mice than in those of the *Hexb*+/? mice, and CR noticeably reduced the number of apoptotic cells in the *Hexb*−/− mice (unpublished observations). Further studies will be necessary to determine the extent of the anti-inflammatory effects of CR in SD and in other ganglioside storage diseases.

Our findings in the mice with SD support our previous studies in mice with epilepsy and brain cancer showing that mild to moderate CR reduces blood glucose and elevates ketone bodies and that these changes are accurate biomarkers of CR (Greene et al., 2001; Seyfried et al., 2003; Mantis et al., 2004; Seyfried and Mukherjee, 2005). The mature brain derives almost all of its energy from the aerobic oxidation of glucose under normal physiological conditions but will oxidize ketone bodies (β-OHB and acetoacetate) for energy during fasting or CR (Owen et al., 1967; Clarke and Sokoloff, 1999; Greene et al., 2001; Mantis et al., 2004). The metabolism of ketone bodies for energy is bioenergetically more efficient than the metabolism of glucose and also reduces oxygen free radical production, because the cytosolic free NAD^+/NADH concentration couple is in near-equilibrium with the glutathione couple (Veech, 2004; Masuda et al., 2005). Oxygen free radicals contribute to tissue inflammation, so we suggest that the energy transition from glucose to ketone bodies contributes to the antiinflammatory and neuroprotective effects of CR. This energy transition might also elevate brain-derived neurotrophic factor (BDNF) and Sir2, which have neuroprotective and anti-inflammatory properties (Maswood et al., 2004; Cohen et al., 2004). We also do not exclude the possibility that pro-inflammatory components in the standard mouse chow might contribute to CNS inflammation in SD mice under AL feeding and that CR simply reduces these components. Further studies involving dietary modifications will be needed to distinguish potential anti-inflammatory mechanisms.

Previous studies showed that NSAIDs improved motor coordination and survival in the *Hexb*−/− mice (Jeyakumar et al., 2004). As with NSAIDs, CR similarly slowed the decline of disease progression during the symptomatic phase of SD. It is interesting to note that both CR and NSAIDs improved behavior without altering the primary disease phenotype, i.e., ganglioside accumulation and storage. In contrast to NSAID therapy, which can involve adverse effects, including stomach ulcers, bruising, fluid retention, kidney problems, headache, dizziness, drowsiness, mouth sores, and skin rashes, CR has no adverse effects (Akarca, 2005; Titchen et al., 2005). Indeed, CR enhances physiological fitness and general heath (Keenan et al., 1999; Greene et al., 2001). Considered together, these findings suggest that CR alone or in combination with low doses of NSAIDs might be a preferred treatment for addressing the inflammatory component of SD.

The CR-induced improvements in survival and behavior of SD mice were not associated with reductions in the total content of gangliosides or in the content of GM2 and GA2. Consistently with these findings, CR did not noticeably reduce cytoplasmic neuronal storage vacuoles or dystrophic neurons. The reductions in cerebrosides and sulfatides in the SD mice are consistent with previous findings of dysmyelination in human patients and in animal models of ganglioside storage disease (Sandhoff et al., 1971; Kaye et al., 1992). CR had no effect on the content or composition of brain cerebrosides or sulfatides. A previous study

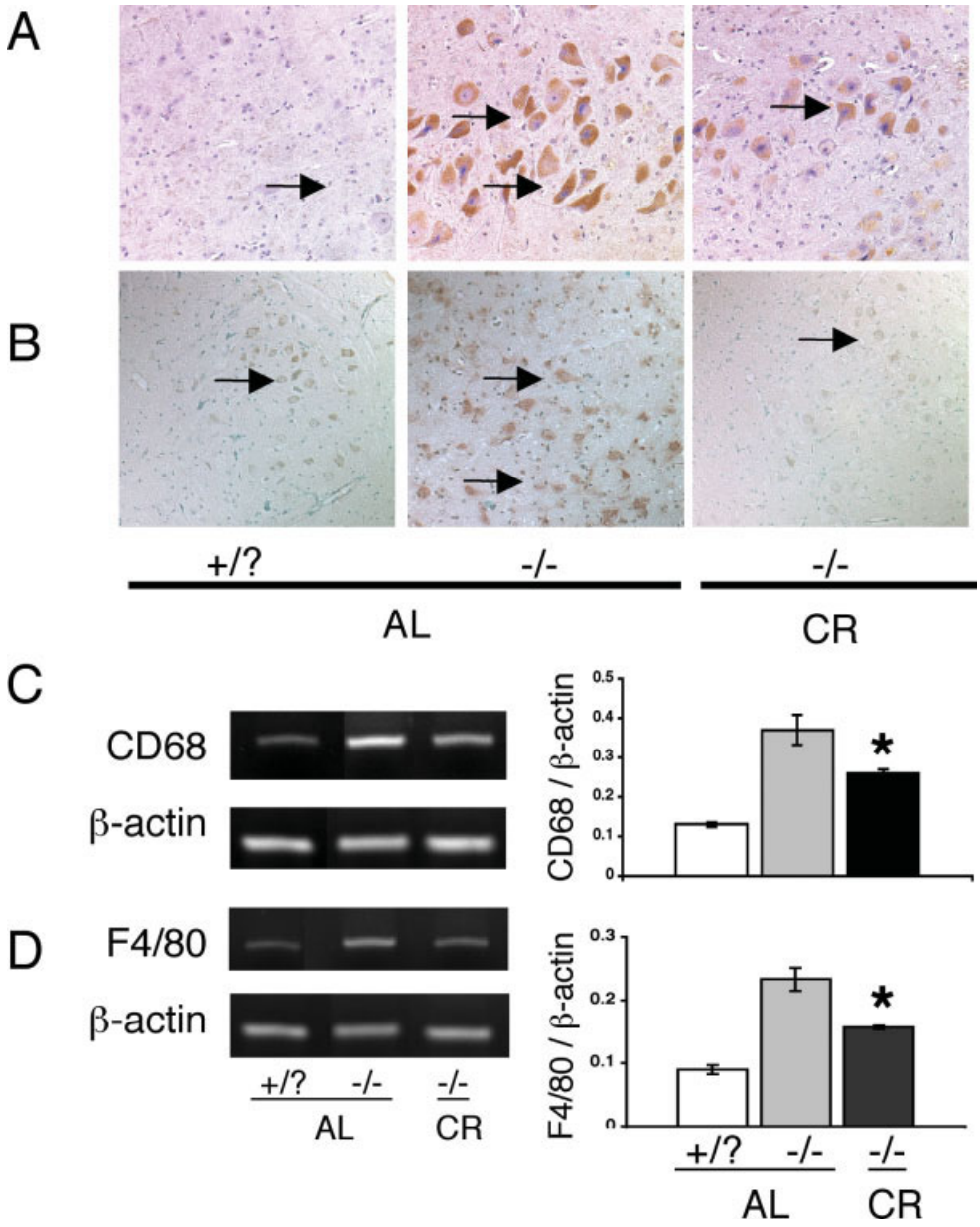

Fig. 6. Influence of CR on CD68 and F4/80 in the cerebral cortex of adult *Hexb* mice. CD68 (**A**) and F4/80 (**B**) immunohistochemistry. Images shown are ×200. CD68 (**C**) and F4/80 (**D**) gene expression. The ratios of CD68/β-actin and F4/80/β-actin are expressed as means (±SEM) and three or four mice were analyzed in each group. *Value of the CR-fed *Hexb*−/− mice is significantly different from that of the AL-fed *Hexb*−/− mice at $P < 0.05$. Figure can be viewed in color online via www.interscience.wiley.com.

suggested that phospholipid abnormalities contribute to the neuropathophysiology in SD mice (Buccoliero et al., 2004). With the exception of a slight reduction in phosphatidylcholine content, no noticeable differences were found between control and SD mice for phospholipid distribution. In addition, CR had no noticeable effect on the distribution of most brain lipids. We do not exclude the possibility that CR might influence some brain lipid molecular species, but further studies using gas-liquid chromatography would be needed to support this possibility. Taken together our findings indicate that CR improves behavior and extends longevity without producing marked changes in glycosphingolipid metabolism or in brain lipid distribution.

In summary, our results show that CR is effective in improving motor coordination and extending longevity in *Hexb*−/− mice during the symptomatic phase of SD, when extensive inflammatory processes are occurring. Furthermore, this improvement was observed without changes in brain glycosphingolipid composition or cytoplasmic neuronal vacuoles and was not associated with observable adverse effects. We suggest that the most effective therapeutic strategy for the life-long management of SD and other ganglioside storage diseases should involve combinatorial therapies, to include SRT (iminosugars, i.e., *N*B-DGJ and *N*B-DNJ), ERT (neural stem cells), and anti-inflammatory approaches (CR and NSAIDs).

ACKNOWLEDGMENTS

We thank Purna Mukherjee, Michael Kiebish, Laura Abate, Rena Baek, Meg Palisoul, and Evan Light for technical assistance.

REFERENCES

Akarca US. 2005. Gastrointestinal effects of selective and non-selective non-steroidal anti-inflammatory drugs. Curr Pharm Des 11:1779–1793.

Ando S, Chang NC, Yu RK. 1978. High-performance thin-layer chromatography and densitometric determination of brain ganglioside compositions of several species. Anal Biochem 89:437–450.

Arfi A, Bourgoin C, Basso L, Emiliani C, Tancini B, Chigorno V, Li YT, Orlacchio A, Poenaru L, Sonnino S, Caillaud C. 2005. Bicistronic lentiviral vector corrects beta-hexosaminidase deficiency in transduced and cross-corrected human Sandhoff fibroblasts. Neurobiol Dis 20:583–593.

Austyn JM, Gordon S. 1981. F4/80, a monoclonal antibody directed specifically against the mouse macrophage. Eur J Immunol 11:805–815.

Baek RC, Kasperzyk JL, Platt FM, Seyfried TN. 2004. N-butyldeoxygalactonojirimycin reduces brain ganglioside and GM2 content in neonatal Sandhoff disease mice. J Neurochem 90(Suppl 1):89.

Baek RC, Lee JP, Seyfried TN, Snyder EY. 2005. Neural stem cell transplantation reduces brain GM2 and GA2 content in a mouse model of Sandhoff disease. J Neurochem 94(Suppl 1):21.

Bond TLY, Neumann PE, Mathieson WB, Brown RE. 2002. Nest building in nulligravid, primigravid and primiparous C57BL/6J and DBA/2J mice (Mus musculus). Physiol Behav 75:551–555.

Broida J, Sware B. 1982. Strain-typical patterns of nest building in mice: maternal and experiential influences. Physiol Behav 29:153–157.

Buccoliero R, Bodennec J, Van Echten-Deckert G, Sandhoff K, Futerman AH. 2004. Phospholipid synthesis is decreased in neuronal tissue in a mouse model of Sandhoff disease. J Neurochem 90:80–88.

Chung HY, Kim HJ, Kim KW, Choi JS, Yu BP. 2002. Molecular inflammation hypothesis of aging based on the anti-aging mechanism of calorie restriction. Microsc Res Techniq 59:264–272.

Clarke DD, Sokoloff L. 1999. Circulation and energy metabolism in the brain. In: Siegel GJ, Agranoff BW, Albers RW, Fisher S K, Uhler MD, editors. Basic neurochemistry, 6th ed. New York: Lippincott-Raven. p 637–669.

Cohen HY, Miller C, Bitterman KJ, Wall NR, Hekking B, Kessler B, Howitz KT, Gorospe M, de Cabo R, Sinclair DA. 2004. Calorie restriction promotes mammalian cell survival by inducing the SIRT1 deacetylase. Science 305:390–392.

Denny CA, Kasperzyk JL, Gorham KN, Bronson RT, Seyfried TN. 2005. Caloric restriction extends longevity without altering brain lipid composition or cytoplasmic neuronal vacuoles in Sandhoff mice. J Neurochem 94(Suppl 1):43.

Duan W, Guo Z, Jiang H, Ware M, Li XJ.Mattson MP. 2003. Dietary restriction normalizes glucose metabolism and BDNF levels, slows disease progression, and increases survival in huntingtin mutant mice. Proc Natl Acad Sci U S A 100:2911–2916.

Galjaard H. 1980. Genetic metabolic disease: diagnosis and prenatal analysis. Amsterdam: Elsevier Science Publishers. p 82–121.

Gravel RA, Clarke JTR, Kaback MM, Mahuran D, Sandhoff K, Suzuki K. 1995. The GM2 gangliosidoses. In: Scriver CR, Beaudet AL, Sly WS, Valle D, editors.The metabolic and molecular bases of inherited disease, 7th ed, vol II. New York: McGraw-Hill. p 2839–2879.

Greene AE, Todorova MT, McGowan R, Seyfried TN. 2001. Caloric restriction inhibits seizure susceptibility in epileptic EL mice by reducing blood glucose. Epilepsia 42:1371–1378.

Greene AE, Todorova MT, Seyfried TN. 2003. Perspectives on the metabolic management of epilepsy through dietary reduction of glucose and elevation of ketone bodies. J Neurochem 86:529–537.

Hauser EC, Kasperzyk JL, d'Azzo A, Seyfried TN. 2004. Inheritance of lysosomal acid b-galactosidase activity and gangliosides in crosses of DBA/2J and knockout mice. Biochem Genet 42:241–257.

Hoag WG, Dickie MM. 1968. Nutrition. In: Green EL, editor. Biology of the laboratory mouse,2nd ed. New York: Dover. p 39–43.

Jeyakumar M, Butters TD, Cortina-Borja M, Hunnam V, Proia RL, Perry VH, Dwek RA, Platt FM. 1999. Delayed symptom onset and increased life expectancy in Sandhoff disease mice treated with N-butyldeoxynojirimycin. Proc Natl Acad Sci U S A 96:6388–6393.

Jeyakumar M, Thomas R, Elliot-Smith E, Smith DA, van der Spoel AC, d'Azzo A, Perry VH, Butters TD, Dwek RA, Platt FM. 2003. Central nervous system inflammation is a hallmark of pathogenesis in mouse models of GM1 and GM2 gangliosidosis. Brain 126:974–987.

Jeyakumar M, Smith DA, Williams I, Borja MC, Neville DCA, Butters TD, Dwek RA, Platt FM. 2004. NSAIDs increase survival in the Sandhoff disease mouse: synergy with N-butyldeoxynojirimycin. Ann Neurol 56:642–649.

Kasperzyk JL, El-Abbadi MM, Hauser EC, D'Azzo A, Platt FM, Seyfried TN. 2004. N-butyldeoxygalactonojirimycin reduces neonatal brain ganglioside content in a mouse model of GM1 gangliosidosis. J Neurochem 89:645–653.

Kasperzyk JL, d'Azzo A, Platt FM, Alroy J, Seyfried TN. 2005. Substrate reduction therapy reduces gangliosides content in postnatal cerebrum-brainstem and cerebellum in GM1 gangliosidosis mice. J Lipid Res 46: 744–751.

Kaye EM, Ullman MD, Kolodny EH, Krivit W, Rischert JC. 1992. Possible use of CSF glycosphingolipids for the diagnosis and therapeutic monitoring of lysosomal storage diseases. Neurology 42:2290–2294.

Keenan KP, Ballam GC, Soper KA, Laroque P, Coleman JB, Dixit R. 1999. Diet, caloric restriction, and the rodent bioassay. Toxicol Sci 52:24–34.

Koubova J, Guarente L. 2003. How does calorie restriction work? Genes Dev 17:313–321.

Kritchevsky D. 1999. Caloric restriction and experimental carcinogenesis. Toxicol Sci 52:13–16.

Ledeen RW. 1983. Gangliosides. In: Lajtha A, editor.Handbook of neurochemistry, vol 3. New York: Plenum Publishing Co. p 41–90.

Lee CK, Weindruch R, Prolla TA. 2000. Gene-expression profile of the ageing brain in mice. Nat Genet 25:294–297.

Macala LJ, Yu RK, Ando S. 1983. Analysis of brain lipids by high performance thin-layer chromatography and densitometry. J Lipid Res 24:1243–1250.

Mantis JG, Centeno NA, Todorova MT, McGowan R, Seyfried TN. 2003. Metabolic control of epilepsy in adult EL mice with the ketogenic diet and caloric restriction. Epilepsia 44(Suppl 9):64–65.

Mantis JG, Centeno NA, Todorova MT, McGowan R, Seyfried TN. 2004. Management of multifactorial idiopathic epilepsy in EL mice with caloric restriction and the ketogenic diet: role of glucose and ketone bodies. Nutr Metab 1:11.

Masuda R, Monahan JW, Kashiwaya Y. 2005. D-beta-hydroxybutyrate is neuroprotective against hypoxia in serum-free hippocampal primary cultures. J Neurosci Res 80:501–509.

Maswood N, Young J, Tilmont E, Zhang Z, Gash DM, Gerhardt GA, Grondin R, Roth GS, Mattison J, Lane MA, Carson RE, Cohen RM, Mouton PR, Quigley C, Mattson MP, Ingram DK. 2004. Caloric restriction increases neurotrophic factor levels and attenuates neurochemical and behavioral deficits in a primate model of Parkinson's disease. Proc Natl Acad Sci U S A 101:18171–18176.

Mattson MP. 2003. Gene-diet interactions in brain aging and neurodegenerative disorders. Ann Intern Med 139:441–444.

Micklem K, Rigney E, Cordell J, Simmons D, Stross P, Turley H, Seed B, Mason D. 1989. A human macrophage-associated antigen (CD68) detected by six different monoclonal antibodies. Br J Haematol 73:6–11.

Morgan TE, Xie Z, Goldsmith S, Yoshida T, Lanzrein AS, Stone D, Rozovsky I, Perry G, Smith MA, Finch CE. 1999. The mosaic of brain glial hyperactivity during normal ageing and its attenuation by food restriction. Neuroscience 89:687–699.

Mukherjee P, Sotnikov AV, Mangian HJ, Zhou JR, Visek WJ, Clinton SK. 1999. Energy intake and prostate tumor growth, angiogenesis, and vascular endothelial growth factor expression. JNCI 91:512–523.

Mukherjee P, El-Abbadi MM, Kasperzyk JL, Ranes MK, Seyfried TN. 2002. Dietary restriction reduces angiogenesis and growth in an orthotopic mouse brain tumour model. Br J Cancer 86:1615–1621.

Myerowitz R, Lawson D, Mizukami H, Mi Y, Tifft CJ, Proia RL. 2002. Molecular pathophysiology in Tay-Sachs and Sandhoff diseases as revealed by gene expression profiling. Hum Mol Genet 11:1343–1350.

Neufeld EF. 1991. Lysosomal storage diseases. Annu Rev Biochem 60: 257–280.

Norflus F, Tifft CJ, McDonald MP, Goldstein G, Crawley JN, Hoffmann A, Sandhoff K, Suzuki K, Proia RL. 1998. Bone marrow transplantation prolongs life span and ameliorates neurologic manifestations in Sandhoff disease mice. J Clin Invest 101:1881–1888.

Owen OE, Morgan AP, Kemp HG, Sullivan JM, Herrera MG, Cahill GF. 1967. Brain metabolism during fasting. J Clin Invest 46:1589–1595.

Phaneuf D, Wakamatsu N, Huang JQ, Borowski A, Peterson AC, Fortunato SR, Ritter G, Igdoura SA, Morales CR, Benoit G, Akerman BR, Leclerc D, Hanai N, Marth JD, Trasler JM, Gravel RA. 1996. Dramatically different phenotypes in mouse models of human Tay-Sachs and Sandhoff diseases. Hum Mol Genet 5:1–14.

Pugh TD, Klopp RG, Weindruch R. 1999. Controlling caloric consumption: protocols for rodents and rhesus monkeys. Neurobiol Aging 20:157–165.

Sandhoff K, Kolter T. 2003. Biosynthesis and degradation of mammalian glycosphingolipids. Philos Trans R Soc Lond B Biol Sci 358:847–861.

Sandhoff K, Harzer K, Wassle W, Jatzkewitz H. 1971. Enzyme alterations and lipid storage in three variants of Tay-Sachs disease. J Neurochem 18: 2469–2489.

Sango K, Yamanaka S, Hoffmann A, Okuda Y, Grinberg A, Westphal H, McDonald MP, Crawley JN, Sandhoff K, Suzuki K, Proia RL. 1995. Mouse models of Tay-Sachs and Sandhoff diseases differ in neurologic phenotype and ganglioside metabolism. Nat Genet 11:170–176.

Seyfried TN, Glaser GH, Yu RK. 1978. Cerebral, cerebellar, and brain stem gangliosides in mice susceptible to audiogenic seizures. J Neurochem 31:21–27.

Seyfried TN, Bernard D, Mayeda F, Macala L, Yu RK. 1984. Genetic analysis of cerebellar lipids in mice susceptible to audiogenic seizures. Exp Neurol 84:590–595.

Seyfried TN, Sanderson TM, El-Abbadi MM, McGowan R, Mukherjee P. 2003. Role of glucose and ketone bodies in the metabolic control of experimental brain cancer. Br J Cancer 89:1375–1382.

Seyfried TN, Greene AE, Todorova MT. 2004. Caloric restriction and epilepsy: historical perspectives, relationship to the ketogenic diet, and analysis in epileptic EL mice. In: Stafstrom CE, editor. Epilepsy and the ketogenic diet. Totowa, NJ: Humana Press. p 247–264.

Spindler SR. 2005. Rapid and reversible induction of the longevity, anticancer, and genomic effects of caloric restriction. Mech Ageing Dev 126: 960–966.

Tannenbaum A. 1942. The genesis and growth of tumors: II. Effects of caloric restriction per se. Cancer Res 2:460–467.

Tannenbaum A. 1959. Nutrition and cancer. In: Homburger F, editor. Physiopathology of cancer. New York: Paul B. Hober. p 517–562.

Titchen T, Cranswick N, Beggs S. 2005. Adverse drug reactions to non-steroidal anti-inflammatory drugs, COX-2 inhibitors and paracetamol in a paediatric hospital. Br J Clin Pharmacol 59:718–723.

Veech RL. 2004. The therapeutic implications of ketone bodies: the effects of ketone bodies in pathological conditions: ketosis, ketogenic diet, redox states, insulin resistance, and mitochondrial metabolism. Prostaglandins Leukotrienes Essent Fatty Acids 70:309–319.

Wada R, Tifft CJ, Proia RL. 2000. Microglial activation precedes acute neurodegeneration in Sandhoff disease and is suppressed by bone marrow transplantation. Proc Natl Acad Sci U S A 97:10954–10959.

Weindruch R, Walford RL. 1988. The retardation of aging and disease by dietary restriction. Springfield, IL: Charles C. Thomas. p 436.

Williamson DH, Mellanby J, Krebs HA. 1962. Enzymic determination of D(–)-beta-hydroxybutyric acid and acetoacetic acid in blood. Biochem J 82: 90–96.

Wu YP, Proia RL. 2004. Deletion of macrophage-inflammatory protein 1 alpha retards neurodegeneration in Sandhoff disease mice. Proc Natl Acad Sci U S A 22:8425–8430.